Control of hair growth and follicle size by VEGF-mediated angiogenesis

Kiichiro Yano,[1] Lawrence F. Brown,[2] and Michael Detmar[1]

[1]Cutaneous Biology Research Center, Department of Dermatology, Massachusetts General Hospital and Harvard Medical School, Charlestown, Massachusetts, USA
[2]Department of Pathology, Beth Israel Deaconess Medical Center and Harvard Medical School, Boston, Massachusetts, USA

Address correspondence to: Michael Detmar, Cutaneous Biology Research Center, Department of Dermatology, Massachusetts General Hospital, Building 149, 13th Street, Charlestown, Massachusetts 02129, USA.
Phone: (617) 724-1170; Fax: (617) 726-4453; E-mail: michael.detmar@cbrc2.mgh.harvard.edu.

Received for publication September 12, 2000, and accepted in revised form January 11, 2001.

The murine hair follicle undergoes pronounced cyclic expansion and regression, leading to rapidly changing demands for its vascular support. Our study aimed to quantify the cyclic changes of perifollicular vascularization and to characterize the biological role of VEGF for hair growth, angiogenesis, and follicle cycling. We found a significant increase in perifollicular vascularization during the growth phase (anagen) of the hair cycle, followed by regression of angiogenic blood vessels during the involution (catagen) and the resting (telogen) phase. Perifollicular angiogenesis was temporally and spatially correlated with upregulation of VEGF mRNA expression by follicular keratinocytes of the outer root sheath, but not by dermal papilla cells. Transgenic overexpression of VEGF in outer root sheath keratinocytes of hair follicles strongly induced perifollicular vascularization, resulting in accelerated hair regrowth after depilation and in increased size of hair follicles and hair shafts. Conversely, systemic treatment with a neutralizing anti-VEGF antibody led to hair growth retardation and reduced hair follicle size. No effects of VEGF treatment or VEGF blockade were observed in mouse vibrissa organ cultures, which lack a functional vascular system. These results identify VEGF as a major mediator of hair follicle growth and cycling and provide the first direct evidence that improved follicle vascularization promotes hair growth and increases hair follicle and hair size.

J. Clin. Invest. **107**:409–417 (2001).

Introduction

The hair follicle undergoes a life-long cyclic transformation from a resting (telogen) phase to a growth (anagen) phase with rapid proliferation of follicular keratinocytes and elongation and thickening of the hair shaft, followed by a regression (catagen) phase leading to involution of the hair follicle (1, 2). These cyclic changes involve rapid remodeling of both epithelial and dermal components and have led to the establishment of the murine hair cycle as a prime model for studies of epithelial-mesenchymal interactions, leading to the identification of several important molecular mediators that control epithelial morphogenesis and growth (3). Similar to the interfollicular epidermis, hair follicles are avascular, and we hypothesized that cyclic hair growth is dependent on the induction of angiogenesis to meet the increased nutritional needs of hair follicles during the anagen phase of rapid cell division. The growing hair follicle is surrounded by blood vessels that have been thought to arise from the deep dermal vascular plexus, and modulation of skin vascularization and perfusion has been previously observed during the hair cycle and in some human diseases characterized by hair loss (4–8). Moreover, it has been demonstrated that anagen hair follicles, similar to the interfollicular epidermis, possess angiogenic properties in experimental in vivo models of angiogenesis (9). However, the biological importance of angiogenesis for hair growth and the molecular mechanisms controlling vascularization of hair follicles have remained unknown.

VEGF plays an important role in mediating angiogenesis during development, as well as in a number of inflammatory and neoplastic diseases that are associated with neovascularization (10). Originally identified as a tumor cell–derived factor that induced vascular hyperpermeability to plasma proteins (11), and therefore named "vascular permeability factor," subsequent studies characterized VEGF as an endothelial cell–specific mitogen. VEGF is a homodimeric, heparin-binding glycoprotein occurring in at least four isoforms of 121, 165, 189, and 201 amino acids, due to alternative splicing (12, 13). VEGF binds to two type III tyrosine kinase receptors on vascular endothelial cells, Flt-1 and KDR/Flk-1 (10). VEGF165 also binds to the neuropilin receptor on endothelial and other cells (14). In vivo, VEGF enhances microvascular permeability (11) and angiogenesis (15, 16). Previously, we have identified VEGF as an angiogenesis factor of major importance for skin vascularization. VEGF expression is upregulated in the hyperplastic epidermis of psoriasis (17), in healing wounds (18), and in other skin diseases characterized by enhanced angiogenesis (19, 20), and targeted overexpression of VEGF in the epidermis of transgenic mice resulted in enhanced skin vascularization with

increased numbers of tortuous and leaky blood vessels (21). Based on these findings, we hypothesized that VEGF might also play an important role in the control of perifollicular vascularization during hair cycling. To investigate perifollicular vascularization during the murine hair cycle and to characterize the biological role of VEGF for follicle growth and cycling, we studied the physiological first postnatal hair cycle and the depilation-induced, synchronized hair cycle in adult mice (22).

We report here that pronounced vascular remodeling occurs during the murine hair cycle, with a more than fourfold increase in perifollicular vessel size during the anagen growth phase and a rapid decrease during catagen and telogen. The changes in vessel size coincided temporally with cyclic changes in follicle size, and perifollicular angiogenesis was temporally and spatially correlated with upregulation of VEGF mRNA expression by follicular keratinocytes of the outer root sheath. Importantly, transgenic overexpression of VEGF in outer root sheath keratinocytes resulted in enhanced perifollicular vascularization, accelerated hair regrowth after depilation, and increased size of vibrissa follicles, hair follicles, and hair shafts. Conversely, blockade of VEGF by systemic treatment with a neutralizing anti-VEGF antibody led to hair growth retardation and to size reduction of hair follicles. These results identify an important role of VEGF in hair biology and might have potential implications for antiangiogenic therapies targeted at inhibition of VEGF, as well as for disorders of hair growth that are characterized by miniaturization of hair follicles.

Methods

Induced adult hair cycle and first postnatal hair cycle. The adult hair cycle was induced in the backskin of 8-week-old female C57BL/6 mice (Charles River Laboratories, Wilmington, Massachusetts, USA) by depilation as described (22), leading to synchronized development of anagen hair follicles. Tissues were obtained at days 1, 3, 5, 8, 12, 18, and 22 after depilation (three mice per time point), encompassing hair development from early anagen to telogen. Tissues were also obtained at different time points (postnatal days 1, 3, 5, 8, 12, 18, and 22; three mice per time point) of the physiological first postnatal hair cycle. Backskin was harvested parallel to the paravertebral line, and the distinct phases of hair follicle development were determined as described (2, 23, 24). Skin samples were either snap-frozen in liquid nitrogen or fixed in 4% paraformaldehyde and embedded in paraffin as described (25). All animal studies were approved by the Massachusetts General Hospital Subcommittee on Research Animal Care.

Hair cycle studies in VEGF transgenic mice. VEGF transgenic mice were established by using a keratin 14 promoter expression cassette to target murine VEGF164 expression to basal epidermal keratinocytes and outer root sheath keratinocytes of hair follicles. The establishment and the phenotypic characterization of VEGF transgenic mice have been previously reported (17). The induced hair cycle was studied in ten 8-week-old VEGF transgenic mice and in ten age-matched wild-type littermates as described above, and tissues were obtained at day 12 ($n = 5$) and day 15 ($n = 5$). Postnatal hair development was studied in five VEGF transgenic mice and five wild-type littermates, and tissues were obtained at postnatal day 15 (late anagen).

Anti-VEGF antibody treatment and Miles vascular permeability assays. Eight-week-old female C57BL/6 mice were injected intraperitoneally with 50 μg of a goat anti–mouse VEGF neutralizing antibody (R&D Systems Inc., Minneapolis, Minnesota, USA; $n = 8$) or with 50 μg of normal goat IgG ($n = 8$) 1 day prior to depilation and thereafter twice weekly. Mice were sacrificed after 12 days ($n = 4$) and 18 days ($n = 4$), and tissues were processed as described above. To confirm the neutralizing activity of the anti-VEGF antibody in vivo, Miles microvascular permeability assays were performed in mice and guinea pigs as previously described (26), using 50 ng of murine VEGF164 for intradermal injections.

Immunohistochemistry and computer-assisted morphometric analysis of perifollicular blood vessels. Immunohistochemical stainings were performed on 5-μm frozen sections as described (27), using a monoclonal rat anti–mouse CD31 antibody (PharMingen, San Diego, California, USA). Representative sections obtained from three mice for each time point were analyzed, using a Nikon E-600 microscope (Nikon Inc., Melville, New York, USA). Images were captured with a Spot digital camera (Diagnostic Instruments Inc., Sterling Heights, Michigan, USA), and morphometric analyses were performed using the IP-LAB software (Scanalytics Inc., Fairfax, Virginia, USA) as described (28). Three different fields in each section were examined at ×60 magnification, and the number of vessels per square millimeter, the average vessel size, and the relative area occupied by blood vessels were determined within an area of 30 μm distance from individual hair follicles. The two-sided unpaired *t* test was used to analyze differences in microvessel density and vascular size. Endothelial cell proliferation was studied by intraperitoneal injection of mice with 5-bromodeoxyuridine (BrdU; 250 mg per kilogram of body weight) 2 hours prior to sacrifice, followed by double immunofluorescence staining with anti-BrdU (PharMingen) and anti-CD31 antibodies (25). Apoptotic endothelial cells were detected by double immunofluorescence, using the Fluorescein-FragEL DNA fragmentation detection kit (Oncogene Research Products, Cambridge, Massachusetts, USA) and an FITC-labeled anti-CD31 antibody.

Measurement of skin thickness and of hair follicle size. Hematoxylin-and-eosin (H&E) stainings were performed on 5-μm paraffin sections of tissues obtained from the first postnatal hair cycle (three mice per time point) and from the induced adolescent hair cycle (three mice per time point). Five representative sections for each sample were analyzed, using a Nikon E-600 microscope (Nikon Inc.). Epidermal, dermal, and subcutaneous thickness was measured in digital images of H&E-stained sections

using the IP-LAB software. The thickness of hair follicles was measured in H&E-stained sections at the level of the largest diameter ("Auber's line") of hair bulbs with clearly visible dermal papilla (50 hair follicles for each time point), using the IP-LAB software. Statistical analyses were performed using the two-sided unpaired Student's *t* test. The diameter of vibrissa follicles was determined in three 8-week-old VEGF transgenic mice and in three age-matched wild-type controls. Eighteen vibrissae per mouse were evaluated, and the follicle thickness was measured at the level of the largest diameter as above. For measurements of hair thickness, hairs were plucked at the end of the second physiological hair cycle from the backs of 12-week-old VEGF transgenic mice ($n = 3$) and of age-matched wild-type controls ($n = 3$). Hairs were placed on glass slides, embedded in OCT compound, and evaluated under a Nikon E-600 microscope. Hair thickness was determined at the widest point of the hair shaft in digital images of awl hair (short, non-curved hair) obtained from VEGF transgenic ($n = 50$ awl hairs) or wild-type ($n = 50$ awl hairs) mice.

In situ hybridization. In situ hybridization was performed on 5-μm paraffin sections as described (27). Antisense and sense single-stranded ^{35}S-labeled RNA probes for VEGF were prepared from a 393-bp rat VEGF cDNA fragment (21). VEGF mRNA expression was quantitated in five sections each obtained from three mice for each time point by counting individual photographic grains over follicular keratinocytes as described (19), and biopsies were scored as negative (0–1 grains per cell; score = 0), weakly positive (2–5 grains per cell; score = 1), moderately positive (6–10 grains per cell; score = 2), or strongly positive (>10 grains per cell; score = 3).

Vibrissa organ cultures. Whisker pads were isolated from 5-week-old female C57BL/6 mice as described and were shortly immersed in 70% ethanol in PBS, followed by incubation in William's E medium containing 400 U/ml penicillin, 400 μg/ml streptomycin, and 1 μg/ml Fungizone (Life Technologies, Rockville, Maryland, USA) for 10 minutes. Vibrissa follicles in the early- or mid-anagen growth phase were isolated under a dissecting microscope, and the part of the hair shaft that extended over the epidermal surface was cut off. Follicles were then plated on nylon membranes (ICN Pharmaceuticals, Irvine, California, USA) in William's E medium alone ($n = 8$), in medium containing 50 ng/ml recombinant murine VEGF (R&D Systems Inc.; $n = 6$), or in medium containing 5% FBS ($n = 8$). In an additional experiment, follicles were incubated with 5 μg/ml of a neutralizing goat anti–mouse VEGF antibody ($n = 7$; the same antibody as used for the in vivo studies described above) or with 5 μg/ml of normal goat IgG ($n = 8$). Media were replaced by fresh media after 2 days, and follicles were incubated over a total period of 4 days. After 4 days, the length of the outgrowing hair shafts was determined by image analysis of digital pictures, using the IP-LAB software. Data are expressed as means ± SD of in vitro hair growth; statistical analyses were performed using the two-sided unpaired Student's *t* test.

Results

Association of hair cycling with cyclic perifollicular angiogenesis. We first studied angiogenesis during depilation-induced, synchronized adult hair cycling (22) by computer-assisted morphometric analyses of back skin sections stained for CD31, an endothelial junction molecule (29). Tissue samples were obtained over a 22-day period that covered all phases of the murine hair cycle from early anagen to telogen (2, 23, 24). A more than fourfold increase in perifollicular vessel size was observed during the late anagen growth phase of the adult hair cycle, as compared with early anagen (Figure 1a), followed by complete reduction to pre-anagen sizes during the catagen and telogen phases (Figure 1, b and f). In contrast, the vessel density, defined as the number of vessels per area unit, was not significantly altered during the hair cycle (Figure 1g). The percentage of perifollicular area covered by vessels increased from 4.1% to 15.9% during the anagen phase and was reduced to 2.9% in telogen (Figure 1e). Similar findings were observed during the physiological first postnatal hair cycle (data not shown). On postnatal day 1 (P1), early anagen follicles were surrounded by small blood vessels with an average size of 148 μm^2, covering 5.9% of the surface area. During late anagen (P12), large, elongated, and dilated vessels were observed surrounding the elongated hair follicles, covering 17.1% of the surface area. A significant reduction in perifollicular vessel sizes to 343 μm^2 was detected during the catagen involution phase (P18) with a concomitant reduction in the surface area covered by vessels to 8.8%. The average vessel size was further reduced to 108 μm^2 in the telogen resting phase with vessels covering only 3.5% of the surface area. These results reveal an identical pattern of perifollicular vascularization during the induced adult hair cycle and the physiological postnatal hair development. Double immunofluorescence stainings for CD31 and BrdU detected proliferating perifollicular endothelial cells throughout the anagen growth phase of the induced hair cycle (Figure 1c), whereas no endothelial proliferation was observed during catagen and telogen. Conversely, apoptotic endothelial cells were selectively detected in perifollicular vessels during the catagen involution phase (Figure 1d). These results establish the murine hair cycle as an easily accessible in vivo system where physiological modulation of angiogenesis can be studied.

Temporal association of perifollicular angiogenesis with cyclic changes of follicle size and cutaneous thickness. We next examined whether the vascular remodeling observed during the anagen growth phase was temporally associated with increases in the size of hair follicles and in the thickness of the overlying epidermis or of the dermis and subcutis. The thickness of interfollicular epidermis significantly increased from day 1 to day 3 (early anagen) of the induced adult hair cycle, and reached a maximum thickness of 54.5 μm on day 5, followed by a steep decline during mid- to late anagen with a further reduction during telogen (Figure 1h). In contrast, cutaneous thickness (dermis and subcutis) steadily increased from early anagen to reach a peak in late anagen, followed by

Figure 1
Pronounced vascular changes during the induced murine hair cycle. (**a** and **b**) CD31 immunostains demonstrate a marked increase in perifollicular vascularization during late anagen (day 12, **a**) with subsequent regression of blood vessels during catagen and telogen (day 22, **b**). (**c**) Detection of proliferating endothelial cells (arrowheads) in perifollicular vessels during the anagen growth phase. Proliferating cells are depicted in red (BrdU), endothelial cells in green (CD31). (**d**) Endothelial cell apoptosis (arrowheads) was detectable in perifollicular vessels during the catagen involution phase. Apoptotic cells are depicted in green, endothelial cells in red. Asterisks indicate the location of hair bulbs. Scale bars = 100 μm. Computer-assisted image analysis revealed significant cyclic changes of relative areas covered by vessels (**e**) and of the average vessel size (**f**), with a more than fourfold increase during anagen ($P < 0.001$) and a decrease to early anagen levels during catagen and telogen. (**g**) Vessel densities were not significantly changed during the hair cycle. Vascular changes were temporally associated with cyclic changes of hair follicle size (**i**) and dermal thickness (**j**), but not of epidermal thickness (**h**). H&E-stained sections were evaluated as described in Methods. Data are expressed as means ± SD of three independent experiments. $^{A}P < 0.05$; $^{B}P < 0.01$; $^{C}P < 0.001$ (increase over early anagen). EA, early anagen; MA, mid-anagen; LA, late anagen; C, catagen; T, telogen; D, day.

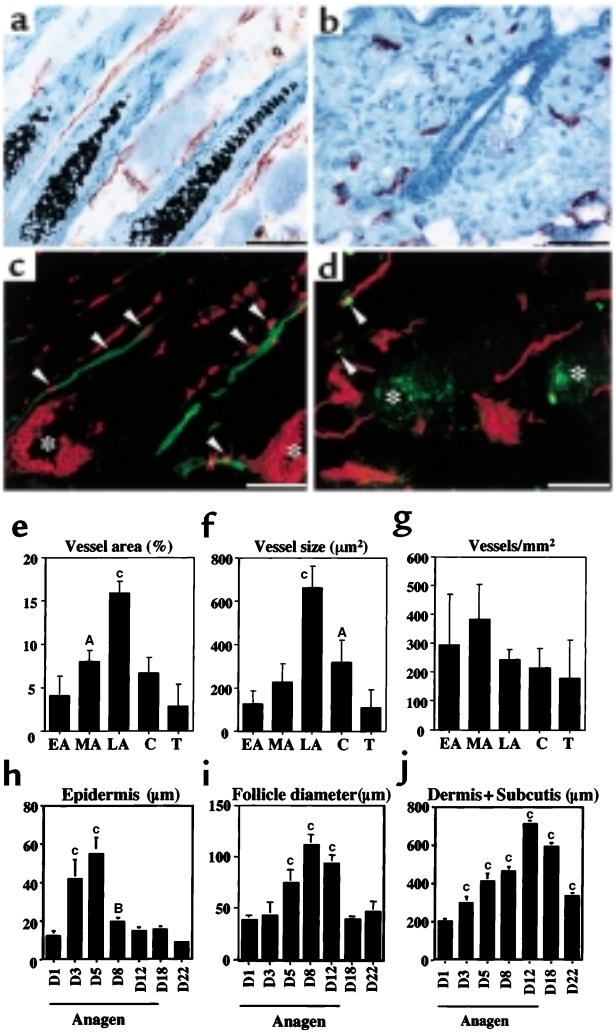

a decline during catagen and telogen (Figure 1j), coinciding with cyclic changes of hair follicle size (Figure 1i). Similar results were obtained during the first postnatal hair cycle. The exact temporal coincidence of changes in follicle size, cutaneous (but not epidermal) thickness, and perifollicular vascularization suggested that the angiogenic stimulus was derived from either the hair follicle itself or the surrounding dermis and subcutis, but not from the interfollicular epidermis.

Upregulation of follicular VEGF expression during the anagen growth phase. Because we had previously identified VEGF as an important mediator of skin angiogenesis (17, 30), we next examined, by in situ hybridization, the spatiotemporal expression pattern of VEGF mRNA during induced hair cycling. Whereas little VEGF mRNA expression was detected in early anagen (day 1) hair follicles or in interfollicular epidermal keratinocytes, VEGF mRNA was highly expressed in follicular keratinocytes during mid-anagen (days 5 and 8), predominantly in the middle third of hair follicles (Figure 2a) where perifollicular angiogenesis was most prominent. In contrast, little or no VEGF mRNA expression was detected in the surrounding dermis and subcutis and in dermal papilla cells. When we correlated VEGF mRNA expression levels with the cyclic changes of perifollicular vascularization, we found that modulations of VEGF expression preceded vascular changes by an interval of approximately 3 days with a marked decrease of VEGF expression during late anagen, catagen, and telogen (Figure 2b). Identical results were obtained during the physiological first postnatal hair cycle (Figure 2c). Thus, the close spatiotemporal association of follicular VEGF expression and perifollicular angiogenesis strongly suggested an important role of follicle-derived VEGF in the control of hair vascularization.

Enhanced hair growth and follicle size in VEGF transgenic mice. To investigate whether follicular VEGF expression directly promotes hair growth and vascularization, we studied the hair cycle in transgenic mice with selective overexpression of VEGF in basal epidermal keratinocytes and in outer root sheath keratinocytes of hair follicles, targeted by a keratin 14 promoter cassette (17). As early as 10 days after depilation, VEGF-overexpressing mice showed accelerated hair regrowth as compared with wild-type littermates. After 11 days, these differences were more obvious, and the hair appeared both longer and thicker in VEGF transgenic mice (Figure 3, a and b). Histological analysis at days 12 and 15 (late anagen) of the induced hair cycle revealed that hair follicles in VEGF transgenic mice were larger than in wild-type controls, most prominently at the level of the hair bulb (Figure 3, c–f). Image analysis of hair bulbs at the level of the maximum bulb diameter revealed a more than 30% increase in diameter in VEGF transgenic mice at day 12 (Figure 3g) and at day 15 (Figure 3j). Importantly, the thickness of fully developed hair shafts was significantly increased ($P < 0.001$), by more than 30%, in VEGF transgenic mice (Figure 4,

a and b), whereas no differences in length were observed. Hair follicles in VEGF transgenic mice were also enlarged during the growth phase (day 15) of the physiological first hair cycle ($P < 0.05$; data not shown). A more than 40% increase in vessel sizes (Figure 3, h and k) and total vascular mass (Figure 3, i and l) was detected surrounding VEGF-overexpressing hair follicles at days 12 and 15, suggesting that accelerated hair growth and increased hair size were a consequence of VEGF-mediated angiogenesis.

Blockade of VEGF activity inhibits hair growth. We next examined whether VEGF-mediated angiogenesis was essential for the timely growth of hair follicles during the anagen phase. Adult C57BL/6 mice were treated systemically with a neutralizing anti-VEGF antibody, and the hair cycle was induced by depilation 1 day after the first antibody application. The neutralizing activity of the anti-VEGF antibody at the concentrations used was confirmed by its ability to completely inhibit VEGF-induced microvascular leakage in the skin of guinea pigs and of mice, measured in a modified Miles assay (data not shown). During the first 8 days after depilation, no differences in the macroscopic skin appearance were observed in anti-VEGF–treated mice. Thereafter, delayed hair regrowth was apparent in anti-VEGF–treated mice. After 12 days, mice treated with the anti-VEGF antibody still showed bald spots and had an overall reduced hair growth (Figure 5b) as compared with normal hair regrowth in control antibody–treated mice (Figure 5a). Histological analysis revealed that anagen hair follicles in anti-VEGF–treated mice were thinner (Figure 5, c and d) with a more than 30% reduction in bulb diameters (Figure 5e), mainly due to reduced thickness of the follicular epithelium, associated with a significant, more than 40% decrease of perifollicular vascularization (Figure 5, f and g).

Absence of VEGF effects on hair growth and follicle size in vibrissa follicle cultures in vitro. Next we investigated whether VEGF might also directly act on hair follicle cells, in addition to its effects on perifollicular angiogenesis. Therefore, we isolated mouse vibrissae and quantitated hair growth and follicle size in organ cultures in vitro, in the absence of a functioning vascular system. Vibrissa follicles are capable of responding to VEGF, as indicated by the significantly increased ($P < 0.01$) diameter of vibrissa follicles in VEGF transgenic mice (Figure 6b) compared with wild-type mice (Figure 6a). In organ culture, untreated mouse vibrissae showed an average hair shaft outgrowth of approximately 2 mm over a period of 4 days (Figure 6, c and d). Addition of 5% FBS to vibrissa cultures, used as a positive control, resulted in a significant ($P < 0.001$) increase of hair shaft growth, confirming the inducibility of hair growth in this experimental system. In contrast, addition of murine VEGF did not affect the hair growth rate in organ culture. Similarly, incubation with a neutralizing goat anti–murine VEGF antibody did not modify in vitro hair growth, as compared with vibrissa cultures treated with equivalent concentrations of goat IgG (Figure 6, c and d). Moreover, treatment of isolated follicles with VEGF or with anti-VEGF antibody did not significantly modify the size of hair bulbs (data not shown). These results suggest that a functional perifollicular vascular system is necessary for the mediation of VEGF effects on follicle growth.

Discussion

Our findings demonstrate that pronounced angiogenesis occurs during murine hair follicle cycling, that follicle-derived VEGF promotes perifollicular vascularization, hair growth rates, and increased follicle and hair size, that blockade of VEGF-mediated angiogenesis leads to impaired hair growth, and that the effects of VEGF are dependent on a functional vascular system.

Using computer-assisted image analysis (25) of sections stained for the endothelial junction molecule CD31 (29), we found pronounced vascular remodeling during the synchronized hair cycle in adult mice, with

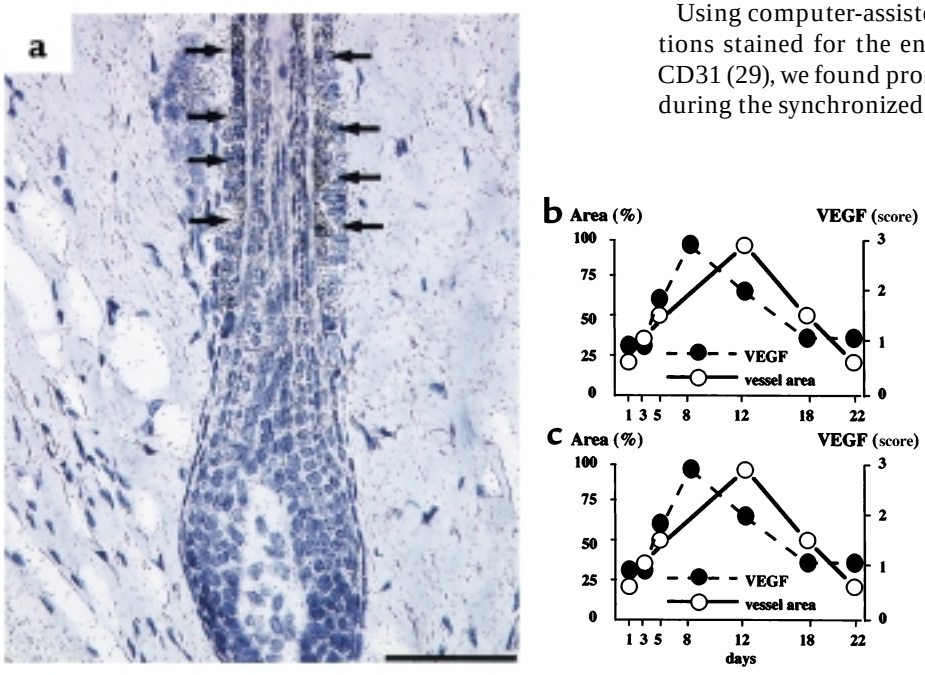

Figure 2
(**a**) In situ hybridization demonstrates strong VEGF mRNA expression in follicular keratinocytes (arrows) during mid-anagen of the induced hair cycle. Scale bar = 50 μm. (**b** and **c**) Temporal correlation of follicular VEGF mRNA expression levels (filled circles) and perifollicular angiogenesis during the induced adult hair cycle (**b**) and the physiological first postnatal hair cycle (**c**). Relative vessel area (open circles) is expressed as percentage of the maximum vessel area detected during late anagen (day 12; compare with Figure 1e).

Figure 3
Accelerated hair regrowth and increased follicle size in VEGF transgenic mice. VEGF transgenic mice showed more and thicker hair at day 11 after depilation (**b**), as compared with wild-type littermates (**a**). Histological analysis of H&E-stained paraffin sections demonstrates increased size of hair bulbs in VEGF transgenic mice at day 12 (**d**) and day 15 (**f**) after depilation, as compared with wild-type (WT) mice at day 12 (**c**) and day 15 (**e**). Scale bars = 100 μm. Hair bulbs in VEGF transgenic mice, measured at the level of the largest diameter, were more than 35% thicker than in wild-type mice at day 12 (**g**) and day 15 (**j**) after depilation. Quantitative analysis of CD31 stains revealed that perifollicular vascularization, assessed as average vessel size (**h**, day 12; **k**, day 15) or relative vessel area (**i**, day 12; **l**, day 15), was significantly increased in VEGF transgenic mice during late anagen. Data are expressed as means ± SD. $^{A}P < 0.01$, $^{B}P < 0.001$, two-sided unpaired Student's *t* test.

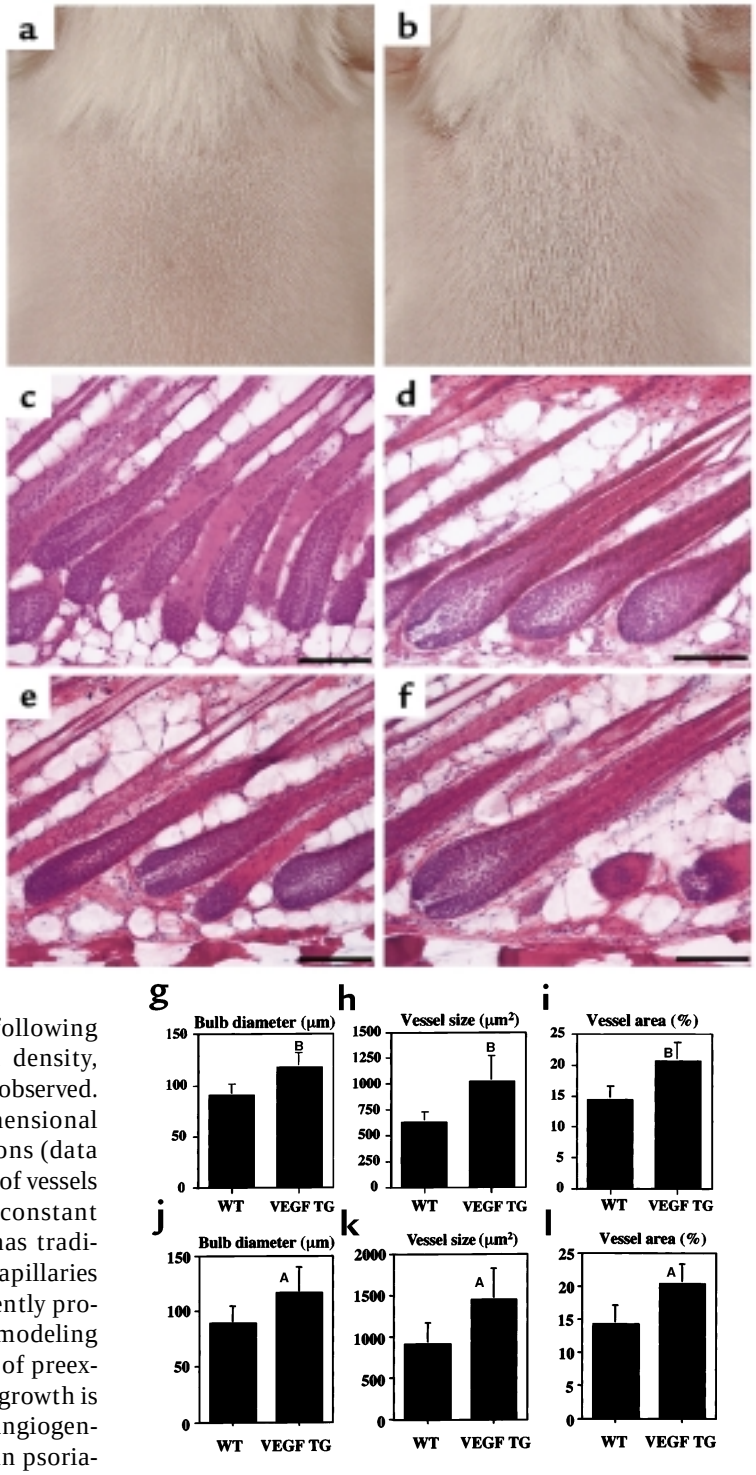

a more than fourfold increase in the average vessel size from early anagen (day 1) to late anagen (day 12). This was followed by regression of vessel sizes, within a time period of 10 days, during the catagen involution and telogen resting phase. These changes in vessel size were associated with significant changes of the relative tissue area covered by vessels. Importantly, comparable changes in perifollicular vascularization were observed during the physiological first postnatal hair cycle, indicating that the increased angiogenesis during the depilation-induced adult hair cycle was not due to a wound response following depilation. No major alterations of vessel density, measured as number of vessels per mm^2, were observed. These findings were supported by three-dimensional reconstruction of serial CD31-stained sections (data not shown), demonstrating that the number of vessels accompanying each hair follicle remained constant during the hair cycle. While angiogenesis has traditionally been defined as the growth of new capillaries from preexisting vessels (31), it has been recently proposed that a second type of angiogenesis ("remodeling type") involves enlargement and elongation of preexisting vessels (32). Our data suggest that hair growth is predominantly associated with remodeling angiogenesis, similar to the angiogenesis that occurs in psoriasis (33), with elongation and enlargement of blood vessels that originate from the upper cutaneous vascular plexus. Angiogenesis during anagen growth was associated with endothelial cell proliferation in perifollicular vessels, whereas apoptotic endothelial cells were selectively detected during the catagen involution phase. Recently, it was suggested that hair follicle growth was associated with increased cutaneous vascular density (34). In this study, only CD31-positive cell aggregates with central lumen formation were evaluated, excluding small blood vessels that are usually found in large numbers during early anagen and telogen (see Figure 1b). Therefore, this approach most likely underestimated the actual vessel density during the resting phase. Taken together, our results establish the murine hair cycle as an easily accessible in vivo system, in addition to the female reproductive system (35, 36) and the mammary gland (37), for studying the molecular mechanisms that control angiogenesis.

Based on our previous findings that VEGF plays a major role in mediating angiogenesis in a large number

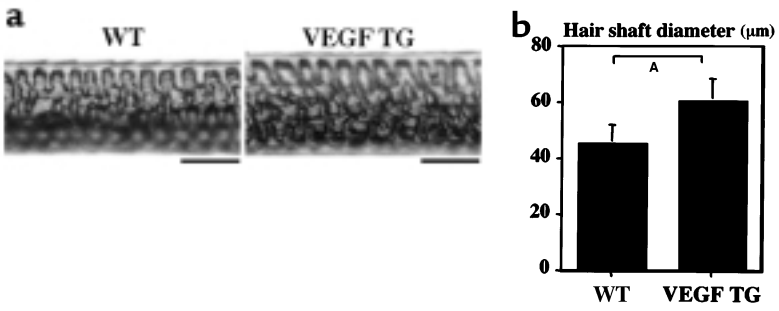

Figure 4
Increased diameter of hair shafts in 12-week-old VEGF transgenic mice (VEGF TG) during late anagen, as compared with wild-type (WT) littermates. (**a**) Light microscopy of unstained plucked awl hair; scale bar = 30 μm. (**b**) Quantitative analysis of hair shafts, measured at the level of their greatest width, revealed a significantly increased hair diameter in VEGF transgenic mice. Data are expressed as means ± SD (n = 50 for each genotype). $^{A}P < 0.001$, two-sided unpaired Student's t test.

of skin diseases (30), we hypothesized that VEGF might also be responsible for the angiogenesis associated with hair cycling. Indeed, semiquantitative in situ hybridization studies revealed that VEGF mRNA expression was selectively upregulated in follicular keratinocytes of the outer root sheath during the early to mid-anagen growth phase, followed by downregulation during the catagen involution phase. In contrast, little or no VEGF mRNA expression was detected in the surrounding dermis or subcutis. Identical results were obtained in the induced adult hair cycle and the physiological first hair cycle. Our findings identify a molecular mechanism by which the growing hair follicle meets its rapidly changing metabolic demands through timed expression of VEGF by follicular keratinocytes, leading to increased perifollicular vascularization. Although it has been reported that cultured dermal papilla cells expressed VEGF in vitro (38–40), we consistently did not detect any upregulation of VEGF mRNA expression in the dermal papilla during the murine hair cycle. These findings are in agreement with a previous report that found the angiogenic activity of the rat vibrissa hair follicle associated with the epithelial hair bulb, but not with the mesenchymal hair papilla (9). Moreover, preliminary studies in a transgenic mouse model for overexpression of the green fluorescent protein gene under control of the VEGF promoter (41) detected VEGF promoter activity selectively in follicular outer root sheath keratinocytes, but not in the dermal papilla (data not shown). These results suggest that VEGF expression levels in cultured papilla cells do not necessarily reflect VEGF expression in vivo, similarly to previous findings in fibroblasts and dermal endothelial cells (42).

To evaluate the biological consequences of follicular VEGF expression for hair growth, we analyzed the induced, synchronized hair cycle in transgenic mice with targeted overexpression of murine VEGF164 in the epidermis and in outer root sheath follicular keratinocytes (21). These mice are characterized by

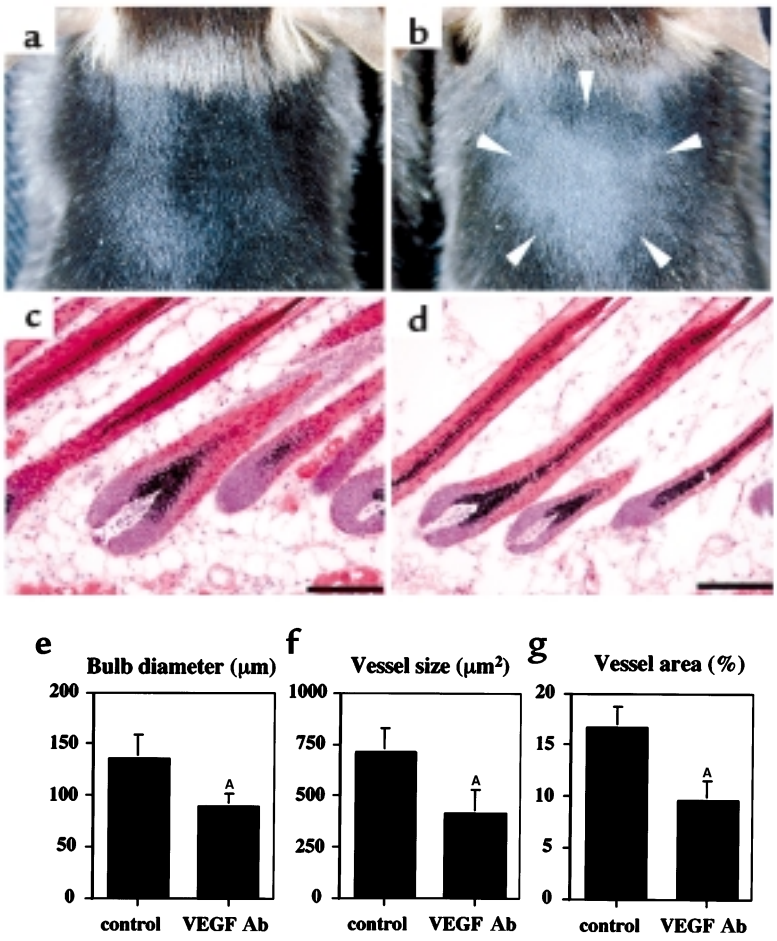

Figure 5
Delayed hair regrowth in C57BL/6 mice after treatment with a neutralizing anti-VEGF antibody. (**a**) At day 12, hair regrowth was complete in control-treated mice, whereas anti-VEGF–treated mice still showed bald spots (**b**, arrowheads). (**c** and **d**) Histological analysis demonstrates diminished thickness of hair bulbs in anti-VEGF–treated mice at day 12 after depilation (**d**), as compared with control mice (**c**). Scale bars = 100 μm. (**e**) Hair bulbs in anti-VEGF–treated mice, measured at the level of the largest diameter, were more than 30% thinner at day 12 after depilation. (**f** and **g**) Quantitative analysis of CD31 stains revealed that perifollicular vascularization, assessed as average vessel size (**f**) or relative vessel area (**g**), was significantly diminished in anti-VEGF–treated mice during late anagen. Data are expressed as means ± SD. $^{A}P < 0.001$, two-sided unpaired Student's t test.

Figure 6
(**a** and **b**) Representative photomicrographs of hematoxylin-stained paraffin sections depict increased size of vibrissa follicles in 8-week-old VEGF transgenic mice (**b**), as compared with age-matched wild-type littermates (**a**). Scale bars = 100 μm. (**c**) Representative photomicrographs of mouse vibrissa organ cultures demonstrate absence of effects of VEGF treatment (V) on the in vitro hair growth rate, as compared with untreated controls (C1). Addition of 5% FBS (P), used as a positive control, resulted in a more than 15% increase in hair growth. Treatment with a neutralizing anti-VEGF antibody (Vab) did not influence in vitro hair growth, as compared with control antibody–treated follicles (C2). (**d**) Quantitative analysis demonstrates significant induction of in vitro hair growth by 5% FBS (P) ($P < 0.001$) but lack of efficiency of VEGF (V) or anti-VEGF antibody (Vab) treatment. Data are expressed as means ± SD. NS, no significant differences between the groups compared. $^{A}P < 0.001$, two-sided unpaired Student's *t* test.

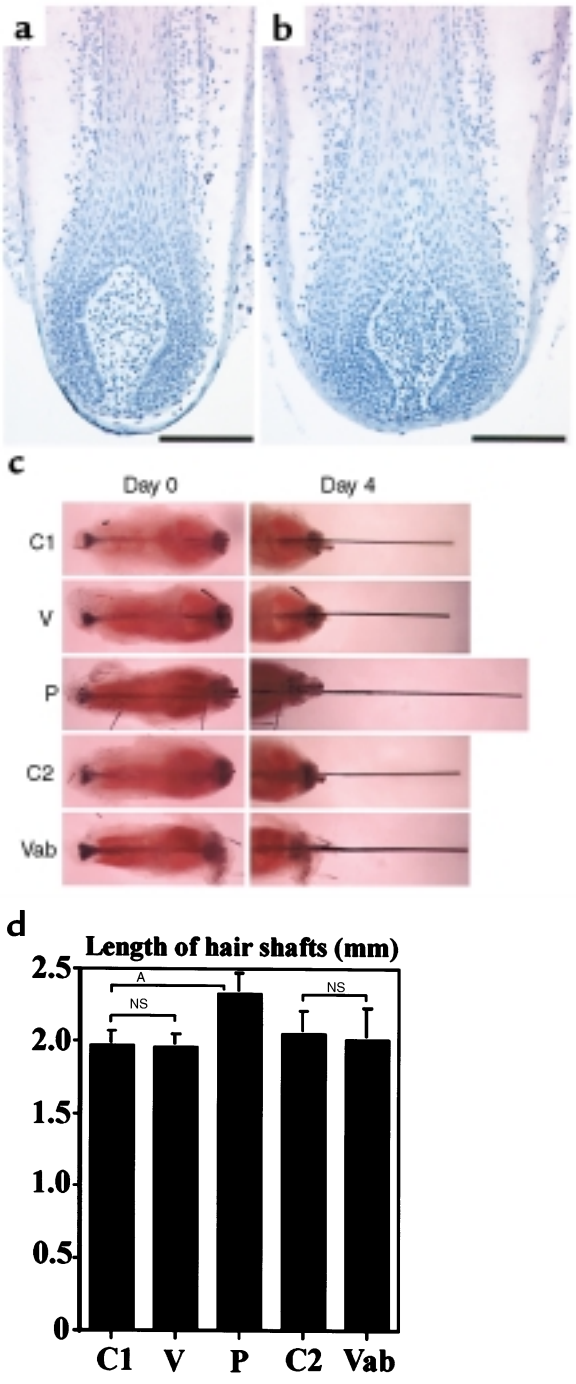

increased cutaneous vascularization and vascular permeability; however, hair growth had not been previously studied in detail. Our study shows that overexpression of VEGF in follicular keratinocytes resulted in accelerated hair regrowth and in increased size of hair follicles, providing the first direct evidence that promotion of angiogenesis can promote hair growth and additionally leads to increased hair thickness. Although vibrissa follicles were also enlarged in VEGF transgenic mice, VEGF treatment did not affect hair growth in organ cultures of mouse vibrissae, in the absence of a functional vascular system. Therefore, our results strongly suggest that the effects of VEGF were mediated indirectly, through induction of perifollicular angiogenesis. The finding that an increase of follicle vascularization over physiological levels led to an increase of follicle size over normal levels suggests that, in addition to improved tissue perfusion, angiogenic blood vessels might also directly influence the growth of the follicle epithelium. In light of the findings that proliferating cutaneous hemangiomas, benign hyperplasias of blood vessel endothelial cells, are regularly associated with significant hyperplasia of the adjacent epidermis (43), these data indicate that increased release of growth factors or diminished production of growth inhibitors by angiogenic endothelial cells might play an additional role in promoting epithelial hyperplasia.

Whereas VEGF inhibition was without effect in isolated mouse vibrissa organ cultures, systemic neutralization of VEGF significantly delayed hair regrowth and resulted in diminished perifollicular vascularization and in reduced size of hair follicles. These findings demonstrate that normal follicle growth and cycling in mice are dependent on VEGF-induced angiogenesis. Impaired vascularization of the hair follicle has been previously suggested to play an important role in the pathogenesis of disorders characterized by hair loss (44–46), including androgenetic alopecia (male-pattern hair loss) where baldness is associated with miniaturization of genetically predisposed follicles (3, 47). Our results support this concept and suggest that some of these disorders may be potential targets for therapies aimed at increasing the vascular support of hair follicles. It remains to be examined whether systemic antiangiogenic therapies, currently developed for treating cancer and other diseases, will also interfere with normal human hair cycling and follicle size or with hair regrowth after polychemotherapy. One has to keep in mind, however, that in contrast to the short duration of the murine hair cycle studied here, the anagen phase of human scalp hair lasts for several years (3) and might show a different sensitivity to reduced vascularization. It also remains to be established whether endogenous

inhibitors of angiogenesis that are normally expressed in the skin, such as thrombospondin-1 and thrombospondin-2 (48), play additional roles in the control of normal hair growth and cycling.

In summary, our results establish an important functional role of VEGF in hair biology and identify a paracrine mechanism by which the proliferative epithelial compartment of the hair follicle, that in itself is not vascularized, induces enhanced vascular support to meet its highly increased nutritional needs during the anagen growth phase. Our data also provide an in vivo proof of concept that normal hair growth and size are dependent on VEGF-induced perifollicular angiogenesis.

Acknowledgments

This work was supported by NIH/National Cancer Institute grants CA-69184 and CA-86410 (to M. Detmar), by American Cancer Society Program Project Grant 99-23901 (to M. Detmar), and by the Cutaneous Biology Research Center through the Massachusetts General Hospital/Shiseido Co. Ltd. Agreement. We thank Donald Senger for help with Miles permeability assays, Myrtha Constant for technical assistance, and Howard Baden, Paolo Dotto, Paul Goetinck, and Ethan Lerner for helpful discussions and critical reading.

1. Chase, H.H. 1954. Growth of the hair. *Physiol. Rev.* **34**:113–126.
2. Hardy, M.H. 1992. The secret life of the hair follicle. *Trends Genet.* **8**:55–60.
3. Paus, R., and Cotsarelis, G. 1999. The biology of hair follicles. *N. Engl. J. Med.* **341**:491–497.
4. Montagna, W., and Ellis, R.A. 1957. Histology and cytochemistry of human skin. XIII. The blood supply of the hair follicle. *J. Natl. Cancer Inst.* **19**:451–463.
5. Durward, A., and Rudall, K.M. 1958. The vascularity and patterns of growth of hair follicles. In *The biology of hair growth.* W. Montagna and R.A. Ellis, editors. Academic Press. New York, New York, USA. 189–218.
6. Stenn, K., Parimoo, S., and Prouty, A.M. 1998. Growth of the hair follicle: a cycling and regenerating biological system. In *Molecular basis of epithelial appendage morphogenesis.* C.-M. Chuong, editor. R.G. Landes Co. Austin, Texas, USA. 111–130.
7. Sholley, M.M., and Cotran, R.S. 1976. Endothelial DNA synthesis in the microvasculature of rat skin during the hair growth cycle. *Am. J. Anat.* **147**:243–254.
8. Ellis, R.A., and Moretti, G. 1959. Vascular patterns associated with catagen hair follicles in the human scalp. *Ann. NY Acad. Sci.* **83**:448–457.
9. Stenn, K.S., Fernandez, L.A., and Tirrell, S.J. 1988. The angiogenic properties of the rat vibrissa hair follicle associate with the bulb. *J. Invest. Dermatol.* **90**:409–411.
10. Dvorak, H.F., Brown, L.F., Detmar, M., and Dvorak, A.M. 1995. Vascular permeability factor/vascular endothelial growth factor, microvascular hyperpermeability, and angiogenesis. *Am. J. Pathol.* **146**:1029–1039.
11. Senger, D.R., et al. 1983. Tumor cells secrete a vascular permeability factor that promotes accumulation of ascites fluid. *Science.* **219**:983–985.
12. Houck, K.A., et al. 1991. The vascular endothelial growth factor family: identification of a fourth molecular species and characterization of alternative splicing of RNA. *Mol. Endocrinol.* **5**:1806–1814.
13. Tischer, E., et al. 1991. The human gene for vascular endothelial growth factor. Multiple protein forms are encoded through alternative exon splicing. *J. Biol. Chem.* **266**:11947–11954.
14. Soker, S., Takashima, S., Miao, H.Q., Neufeld, G., and Klagsbrun, M. 1998. Neuropilin-1 is expressed by endothelial and tumor cells as an isoform-specific receptor for vascular endothelial growth factor. *Cell.* **92**:735–745.
15. Connolly, D.T., et al. 1989. Tumor vascular permeability factor stimulates endothelial cell growth and angiogenesis. *J. Clin. Invest.* **84**:1470–1478.
16. Leung, D.W., Cachianes, G., Kuang, W.-J., Goeddel, D.V., and Ferrara, N. 1989. Vascular endothelial growth factor is a secreted angiogenic mitogen. *Science.* **246**:1306–1309.
17. Detmar, M., et al. 1994. Overexpression of vascular permeability factor/vascular endothelial growth factor and its receptors in psoriasis. *J. Exp. Med.* **180**:1141–1146.
18. Brown, L.F., et al. 1992. Expression of vascular permeability factor (vascular endothelial growth factor) by epidermal keratinocytes during wound healing. *J. Exp. Med.* **176**:1375–1379.
19. Brown, L.F., et al. 1995. Increased expression of vascular permeability factor (vascular endothelial growth factor) in bullous pemphigoid, dermatitis herpetiformis, and erythema multiforme. *J. Invest. Dermatol.* **104**:744–749.
20. Brown, L.F., et al. 1995. Overexpression of vascular permeability factor (VPF/VEGF) and its endothelial cell receptors in delayed hypersensitivity skin reactions. *J. Immunol.* **154**:2801–2807.
21. Detmar, M., et al. 1998. Increased microvascular density and enhanced leukocyte rolling and adhesion in the skin of VEGF transgenic mice. *J. Invest. Dermatol.* **111**:1–6.
22. Paus, R., Stenn, K.S., and Link, R.E. 1990. Telogen skin contains an inhibitor of hair growth. *Br. J. Dermatol.* **122**:777–784.
23. Dry, F.W. 1926. The coat of the mouse (mus musculus). *Journal of Genetics.* **16**:287–340.
24. Davidson, P., and Hardy, M.H. 1952. The development of mouse vibrissae in vivo and in vitro. *J. Anat.* **86**:342–356.
25. Streit, M., et al. 2000. Thrombospondin-1 suppresses wound healing and granulation tissue formation in the skin of transgenic mice. *EMBO J.* **19**:3272–3282.
26. Senger, D.R., Connolly, D.T., Van De Water, L., Feder, J., and Dvorak, H.F. 1990. Purification and NH2-terminal amino acid sequence of guinea pig tumor-secreted vascular permeability factor. *Cancer Res.* **50**:1774–1778.
27. Detmar, M., et al. 2000. Expression of vascular endothelial growth factor induces an invasive phenotype in human squamous cell carcinomas. *Am. J. Pathol.* **156**:159–167.
28. Streit, M., et al. 1999. Thrombospondin-2: a potent endogenous inhibitor of tumor growth and angiogenesis. *Proc. Natl. Acad. Sci. USA.* **96**:14888–14893.
29. Dejana, E., Corada, M., and Lampugnani, M.G. 1995. Endothelial cell-to-cell junctions. *FASEB J.* **9**:910–918.
30. Detmar, M. 1996. Molecular regulation of angiogenesis in the skin. *J. Invest. Dermatol.* **106**:207–208.
31. Risau, W. 1997. Mechanisms of angiogenesis. *Nature.* **386**:671–674.
32. Carmeliet, P. 2000. Mechanisms of angiogenesis and arteriogenesis. *Nat. Med.* **6**:389–395.
33. Braverman, I.M., and Sibley, J. 1982. Role of the microcirculation in the treatment and pathogenesis of psoriasis. *J. Invest. Dermatol.* **78**:12–17.
34. Mecklenburg, L., et al. 2000. Active hair growth (anagen) is associated with angiogenesis. *J. Invest. Dermatol.* **114**:909–916.
35. Iruela-Arispe, M.L., and Dvorak, H.F. 1997. Angiogenesis: a dynamic balance of stimulators and inhibitors. *Thromb. Haemost.* **78**:672–677.
36. Goede, V., Schmidt, T., Kimmina, S., Kozian, D., and Augustin, H.G. 1998. Analysis of blood vessel maturation processes during cyclic ovarian angiogenesis. *Lab. Invest.* **78**:1385–1394.
37. Matsumoto, M., Nishinakagawa, H., Kurohmaru, M., Hayashi, Y., and Otsuka, J. 1992. Pregnancy affects the microvasculature of the mammalian gland in mice. *J. Vet. Med. Sci.* **54**:937–943.
38. Lachgar, S., et al. 1996. Vascular endothelial growth factor is an autocrine growth factor for hair dermal papilla cells. *J. Invest. Dermatol.* **106**:17–23.
39. Lachgar, S., Charveron, M., Gall, Y., and Bonafe, J.L. 1998. Minoxidil upregulates the expression of vascular endothelial growth factor in human hair dermal papilla cells. *Br. J. Dermatol.* **138**:407–411.
40. Kozlowska, U., et al. 1998. Expression of vascular endothelial growth factor (VEGF) in various compartments of the human hair follicle. *Arch. Dermatol. Res.* **290**:661–668.
41. Kishimoto, J., et al. 2000. In vivo detection of human vascular endothelial growth factor promoter activity in transgenic mouse skin. *Am. J. Pathol.* **157**:103–110.
42. Detmar, M., et al. 1997. Hypoxia regulates the expression of vascular permeability factor/vascular endothelial growth factor (VPF/VEGF) and its receptors in human skin. *J. Invest. Dermatol.* **108**:263–268.
43. Bielenberg, D.R., et al. 1999. Progressive growth of infantile cutaneous hemangiomas is directly correlated with hyperplasia and angiogenesis of adjacent epidermis and inversely correlated with expression of the endogenous angiogenesis inhibitor, IFN-beta. *Int. J. Oncol.* **14**:401–408.
44. Levy-Frankel, J., and Juster, E. 1931. Recherche sur le mecanisme physiopathologique de la pelade. *Ann. Dermatol. Syphiligr. (Paris).* **2**:1074–1088.
45. Beurey, J., Weber, M., Bertrand, A., Robert, J., and Mabille, H. 1971. Mesure du debit vasculaire des plaques peladiques au moyen du xenon 133. *Bull. Soc. Fr. Dermatol. Syphiligr.* **79**:176–180.
46. Goldman, C.K., Tsai, J.C., Soroceanu, L., and Gillespie, G.Y. 1995. Loss of vascular endothelial growth factor in human alopecia hair follicles. *J. Invest. Dermatol.* **104**(Suppl. 1):18S–20S.
47. Cormia, F.E., and Ernyey, A. 1961. Circulatory changes in alopecia. *Arch. Dermatol.* **84**:772.
48. Detmar, M. 2000. The role of VEGF and thrombospondins in skin angiogenesis. *J. Dermatol. Sci.* **24**(Suppl. 1):S78–S84.